JOURNAL OF GEOPHYSICAL RESEARCH, VOL. 106, NO. A12, PAGES 30,085–30,097, DECEMBER 1, 2001

The response of the high-latitude ionosphere to the coronal mass ejection event of April 6, 2000: A practical demonstration of space weather nowcasting with the Super Dual Auroral Radar Network HF radars

J. M. Ruohoniemi, R. J. Barnes, R. A. Greenwald, and S. G. Shepherd[1]

The Johns Hopkins University Applied Physics Laboratory, Laurel, Maryland

Abstract. The ionosphere at high latitudes is the site of important effects in space weather. These include strong electrical currents that may disrupt power systems through induced currents and density irregularities that can degrade HF and satellite communication links. With the impetus provided by the National Space Weather Program, the radars of the Super Dual Auroral Radar Network have been applied to the real-time specification ("nowcasting") of conditions in the high-latitude ionosphere. A map of the plasma convection in the northern high-latitude ionosphere is continually generated at the Johns Hopkins University Applied Physics Laboratory (JHU/APL) SuperDARN web site using data downloaded in real time from the radars via Internet connections. Other nowcast items include information on the conditions of HF propagation, the spatial extent of auroral effects, and the total cross polar cap potential variation. Time series of various parameters and an animated replay of the last 2 hours of convection patterns are also available for review. By comparing with simultaneous measurements from an upstream satellite, it is possible to infer the effective delay from the detection of changes in the solar wind at the satellite to the arrival of related effects in the high-latitude ionosphere. We discuss the space weather products available from the JHU/APL SuperDARN web site and their uses by simulating a nowcast of the ionosphere on April 6, 2000, during the arrival of a coronal mass ejection (CME) -related shock. The nowcast convection pattern in particular satisfies a critical need for timely, comprehensive information on ionospheric electric fields.

1. Introduction

The coupling of energy and momentum from the solar wind to the Earth's magnetosphere is a critical link in the chain of events that begins with the ejection of solar mass and energy and ends with the effects in the near-Earth environment that are characterized as space weather. The high-latitude regions are especially sensitive to changes in the solar wind plasma; the first clear sign of the onset of a major geomagnetic disturbance is often seen in the auroral ionosphere. The manner in which the ionosphere responds to solar wind factors has long been studied for scientific insight into the physics of the coupling processes. More recently, it has been realized that the ionosphere at high latitudes can be monitored for comprehensive and timely information on space weather conditions.

The high-latitude ionosphere is closely coupled to the outer magnetosphere by the lines of force of the geomagnetic field. These are highly conducting and allow electric fields to map with little attenuation throughout the magnetospheric–ionospheric volume. The electric fields drive plasma motion (convection) according to $\mathbf{V} = \mathbf{E}\mathrm{x}\mathbf{B}/B^2$, where $\mathbf{V}$ is the plasma velocity, $\mathbf{E}$ is the electric field, and $\mathbf{B}$ is the geomagnetic field. The electric fields generated by the interaction of the solar wind with the magnetosphere result in a large-scale pattern of plasma circulation. Most often this convection pattern carries ionospheric plasma in the antisunward direction across the high polar cap and returns it to the dayside via the dawn and dusk flanks at lower latitudes. Numerous studies have demonstrated the importance of the interplanetary magnetic field (IMF) carried by the solar wind for high-latitude convection [e.g., *Heppner and Maynard*, 1987; *Rich and Hairston*, 1994; *Weimer*, 1995; *Ruohoniemi and Greenwald*, 1996]. The convection electric fields produce strong ionospheric currents that can disrupt power systems, generate irregularities that degrade satellite and HF communications, and affect sensitive systems by redistributing ionospheric ionization and structure throughout the high-latitude regions.

One important aim is the forecasting of disturbances in the near-Earth space environment of concern for human health and technology. It is also important to characterize, by "nowcasting," the current conditions, both as an assessment of immediate risk and for information to update the forecasts. As is the case with conventional weather, distributed measurements of key parameters are necessary to both nowcast and forecast the weather in space.

[1]Now at the Thayer School of Engineering, Dartmouth College, 8000 Cummings Hall, Hanover, NH 03755

Paper number 2000JA000217.
0148-0227/01/2000JA000217$09.00

With the impetus provided by the National Space Weather Program, it has been recognized that accurate determination of ionospheric electric fields in the high-latitude regions would constitute a space weather diagnostic with broad operational application. Ideally, this would include the ability to "image" the convection on global scales with spatial and temporal resolutions sufficient to track all the effects of interest. Information on the electric field would provide a critical test of the comprehensive MHD codes that are being developed to forecast space weather. An analogy can be drawn with terrestrial weather predictions for which distributed measurements of temperature and pressure are assimilated into first-principles computer codes. The success of the predictive efforts will likely hinge on their ability to incorporate "ground truth" measurements of such important parameters as the ionospheric electric field.

One response of the research community to the need for diagnostic measurements has been to adapt the Super Dual Auroral Radar Network (SuperDARN) system to real-time specification of conditions in the high-latitude ionosphere. The primary product of SuperDARN is information on ionospheric electric fields including mapping of the global convection pattern. It also provides information on the occurrence of irregularities and the conditions of HF propagation. SuperDARN consists of longitudinal chains of HF radars in both the Northern and Southern Hemispheres. It is an international collaboration involving teams of scientists and the funding agencies of over a dozen countries [*Greenwald et al.*, 1995]. Only the northern radars possess an extensive real-time capability. Plate 1 shows the overlapping fields of view of these radars, and Table 1 provides a listing of their affiliations. The prototype radar has operated at Goose Bay since 1983, but the multiradar concept of SuperDARN was first realized in 1993 with the establishment of new radars in Kapuskasing and Saskatoon. Since then, the northern chain has grown to eight radars with a ninth scheduled for completion in the summer of 2001.

A recent critical development has been the establishment of Internet links to the radars. This has made it possible to monitor the observations of the radars and process summary data in near real time. Maps of the global convection pattern and related ionospheric products are generated continuously and posted to the Johns Hopkins University/Applied Physics Laboratory (JHU/APL) SuperDARN web site. This ability to nowcast the state of the high-latitude ionosphere on the basis of direct, comprehensive measurements is an important community asset. It also represents the culmination of a broad effort to transition a research tool into an operational space weather service.

Table 1. Affiliations of Northern Hemisphere SuperDARN Radars[a]

Principal Investigator	Institution	Radar
R. A. Greenwald	JHU/APL	Goose Bay
		Kapuskasing
G. J. Sofko	University of Saskatchewan	Saskatoon
		Prince George
J.-P. Villain	CNRS	Stokkseyri
M. Lester	University of Leicester	Hankasalmi
		Pykkvibaer
W. A. Bristow	UAF	Kodiak
T. Kikuchi	CRL	King Salmon

[a]SuperDARN, Super Dual Auroral Radar Network; JHU/APL, The Johns Hopkins University Applied Physics Laboratory; CNRS, Centre National de la Recherche Scientifique; UAF, University of Alaska Fairbanks; CRL, Communications Research Laboratory

The nowcast convection patterns make possible a real-time analysis of the conditions in the polar ionosphere. The extent and magnitude of the plasma flows are shown directly, and the impact of solar wind factors on convection is apparent in the evolution of the patterns. The electric fields can be mapped into the magnetosphere and applied to the study of magnetosphere–ionosphere coupling. Effects in convection are also known to accompany substorm onsets [e.g., *Yeoman et al.*, 1999]. The task of theorists and modelers includes accounting self-consistently for these aspects of solar wind–magnetosphere–ionosphere coupling as they are constrained by electric field observations of this kind. In addition, convection redistributes ionization and structure throughout the high-latitude ionosphere and contributes to the dynamics and energy budget of the neutral atmosphere. An evaluation of these effects as space weather phenomena requires timely, accurate characterization of the electric fields.

In this paper we demonstrate the capabilities of the SuperDARN system for nowcasting the space weather in the high-latitude ionosphere. We also describe some other types of relevant information that can be gleaned from examination of the SuperDARN data. To make this a truly practical demonstration, we have selected a single event and follow its progress through the nowcast at the JHU/APL SuperDARN web site. The selected event relates to the arrival of a shock in the solar wind on April 6, 2000. Fortuitously, the disturbance arrived during office hours in North America, and its significance was quickly appreciated. A movie showing the effect of the arrival of the shock on the SuperDARN observations was posted to the web site and widely viewed. Operation of the large incoherent scatter radar facility at Millstone Hill was initiated on that day partly because of the expansion of the auroral zone to midlatitudes seen in the SuperDARN nowcast.

2. The Solar Wind Shock of April 6, 2000

An M-class solar flare that occurred on April 4 at 1541 UT was accompanied by a halo coronal mass ejection (CME). The associated shock reached the Earth on April 6 near 1640 UT. The shock was followed by a prolonged period of geomagnetic disturbance that included sightings of aurora in the mid-Atlantic states of the United States and in central Japan.

The ACE satellite at an upstream position of 225 R_E was the first to detect the shock in the solar wind. Figure 1 shows time series of the magnetic field data for the 1500–1800 UT interval. Extremely sharp transitions occurred in the y and z components of the IMF at 1604 UT, and its magnitude increased by a factor of 3. The particle data (not shown) indicated a coincident fivefold increase in dynamic pressure with an increase in velocity from 400 to 600 km s^{-1}. Similar effects were recorded by the Wind satellite located 50 R_E

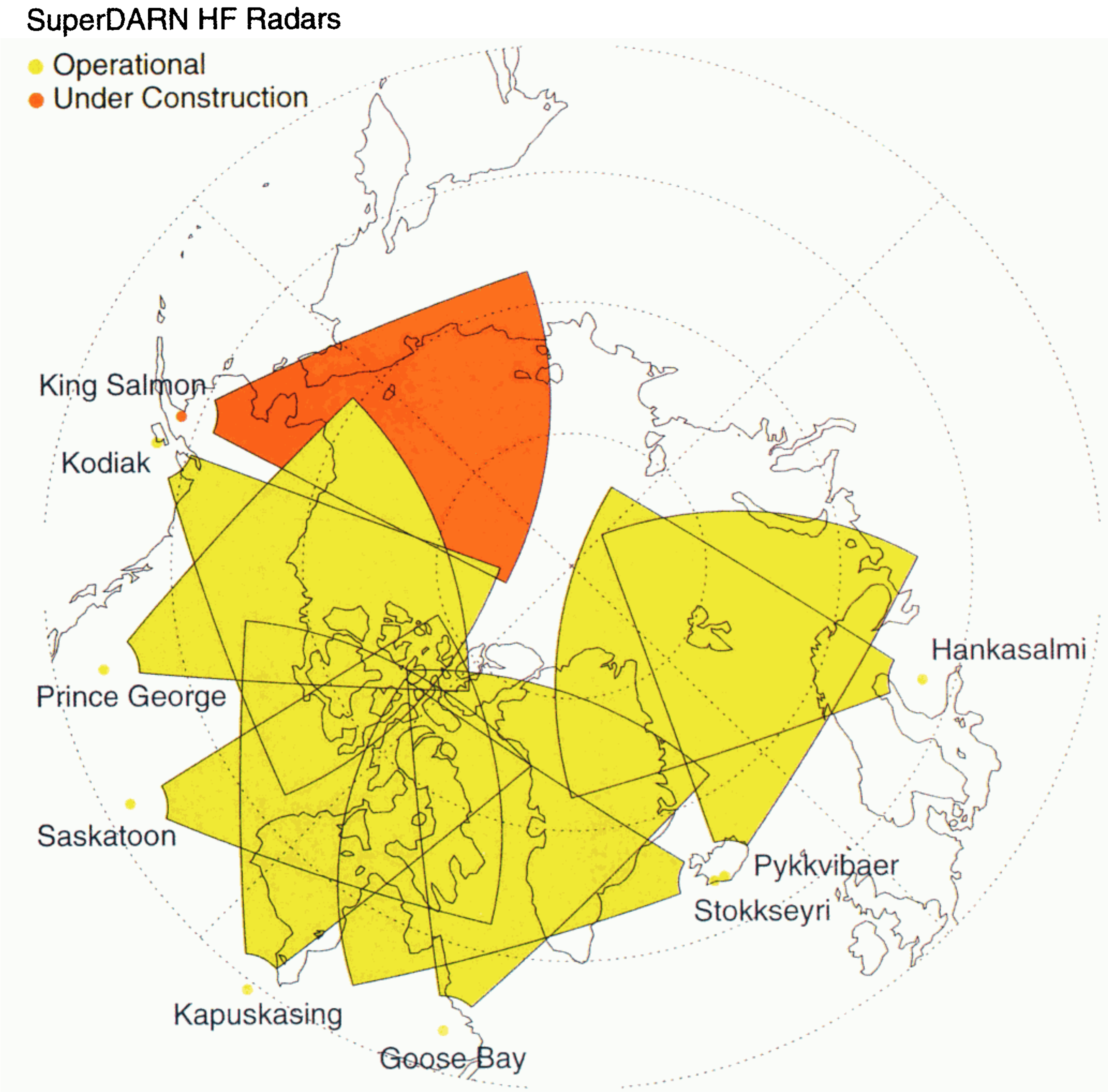

Plate 1. Fields of view of the Super Dual Auroral Radar Network (SuperDARN) HF radars in the Northern Hemisphere.

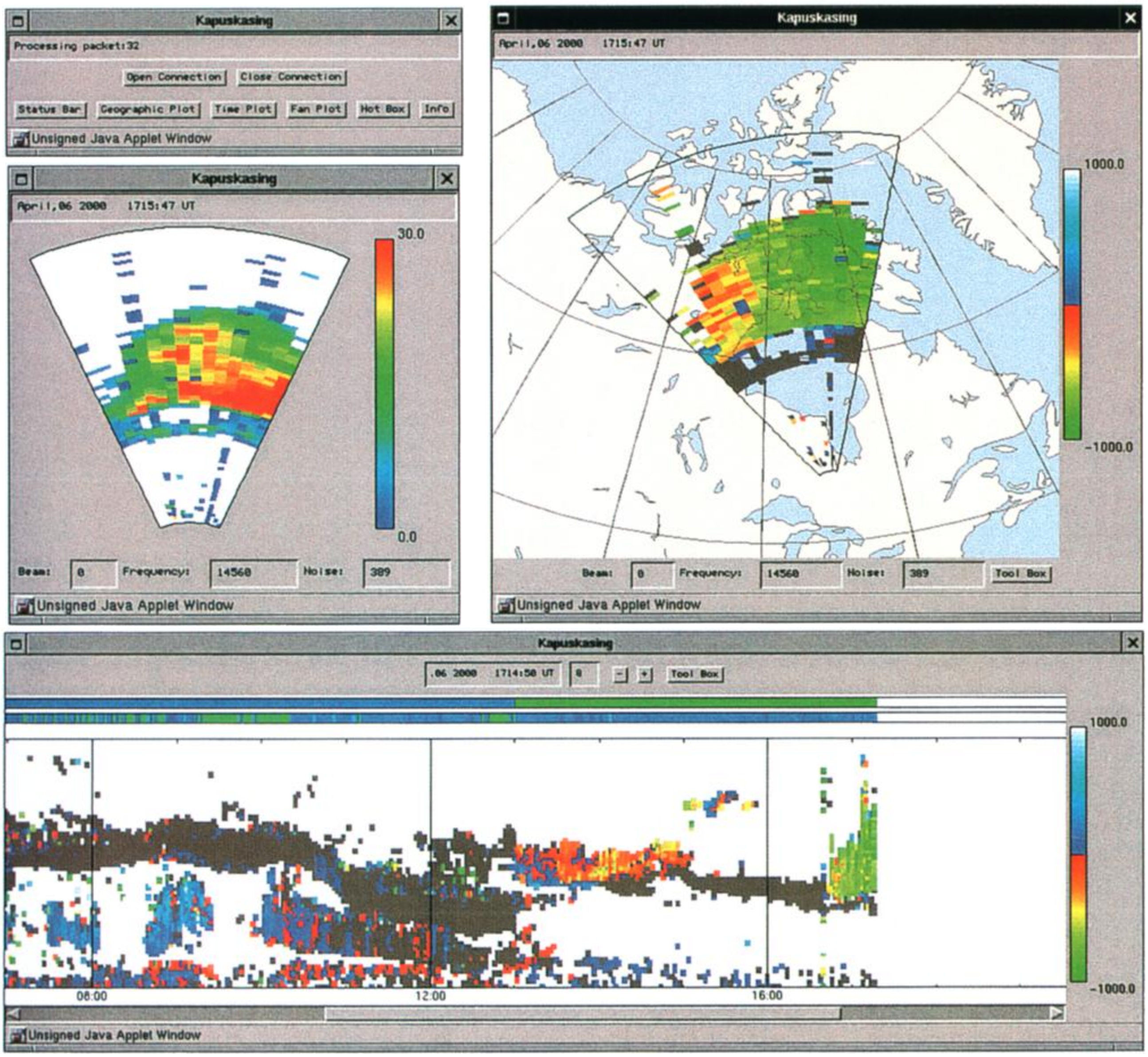

Plate 2. Simulated real-time plots of data from the Kapuskasing HF radar. The particular types of data and format are selected using the pop-up menus. The smaller of the fan plots shows backscattered power in decibels while the larger shows line-of-sight velocity. The gray coding in the velocity plot indicates groundscatter. The lower panel shows a fragment of the time series plot of velocity data for one beam of the radar. The real-time web page includes full-day time series plots of backscattered power, velocity, and spectral width.

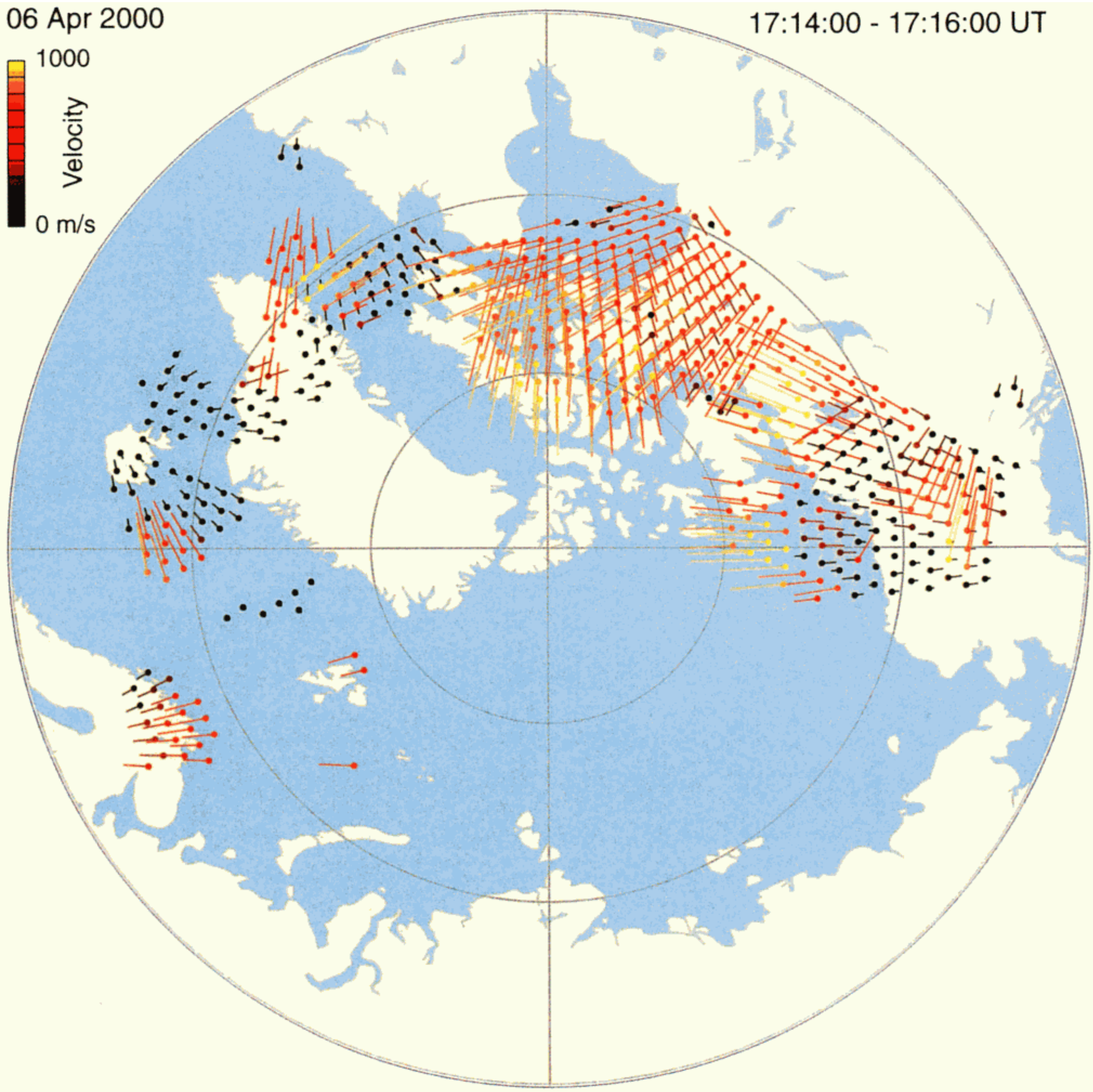

Plate 3. Plot of the line-of-sight SuperDARN velocity data mapped into the global grid for the 2-min scan ending at 1716 UT.

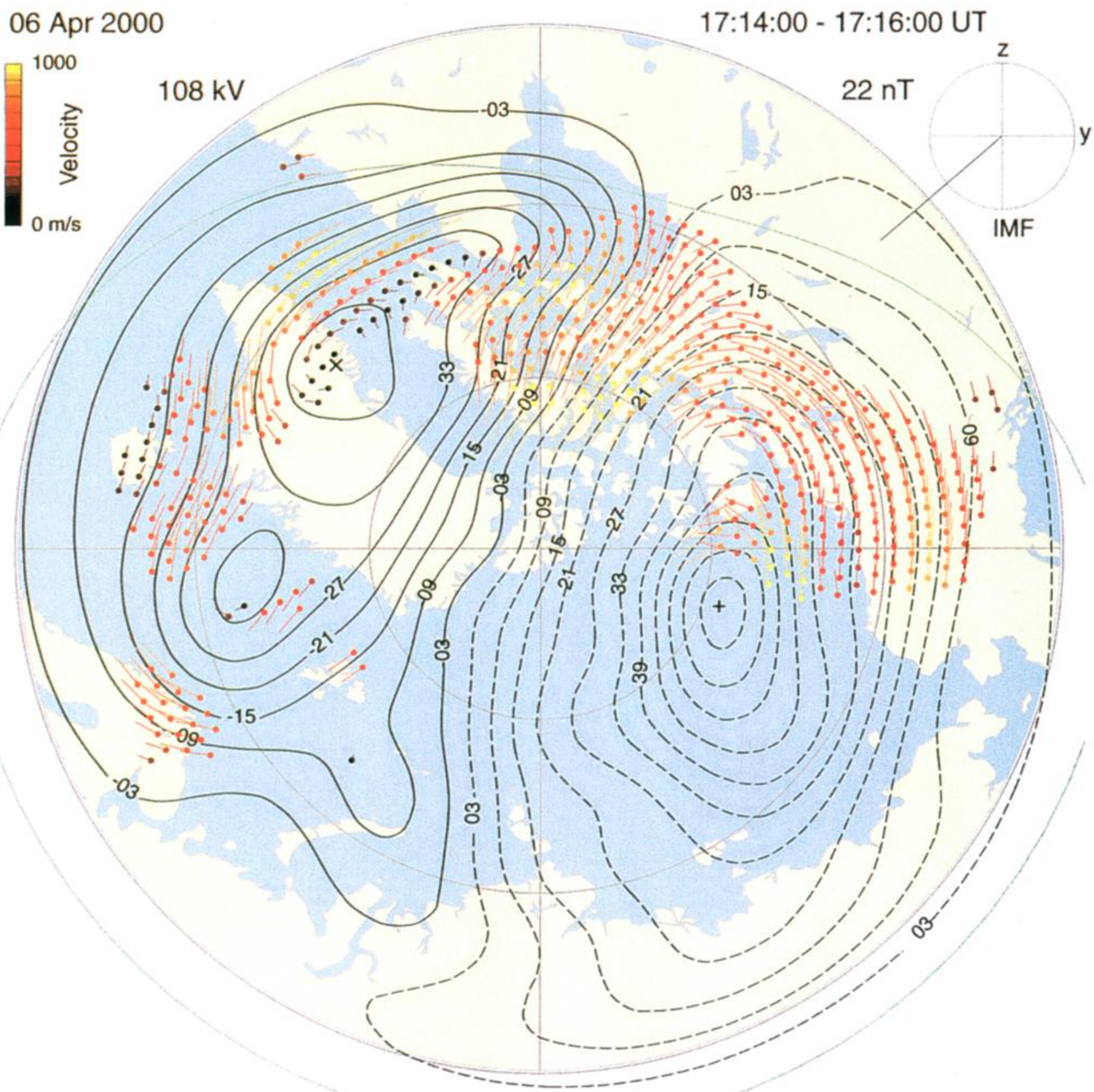

Plate 4. SuperDARN nowcast of the global convection pattern for the scan ending at 1716 UT. The vectors are plotted where supporting velocity data were available from the SuperDARN radars. The smaller insert plot in the upper right-hand corner shows the time-delayed IMF in the GSM *y-z* plane. The positions of the potential extrema are indicated by a plus sign (positive) and an *x* sign (negative).

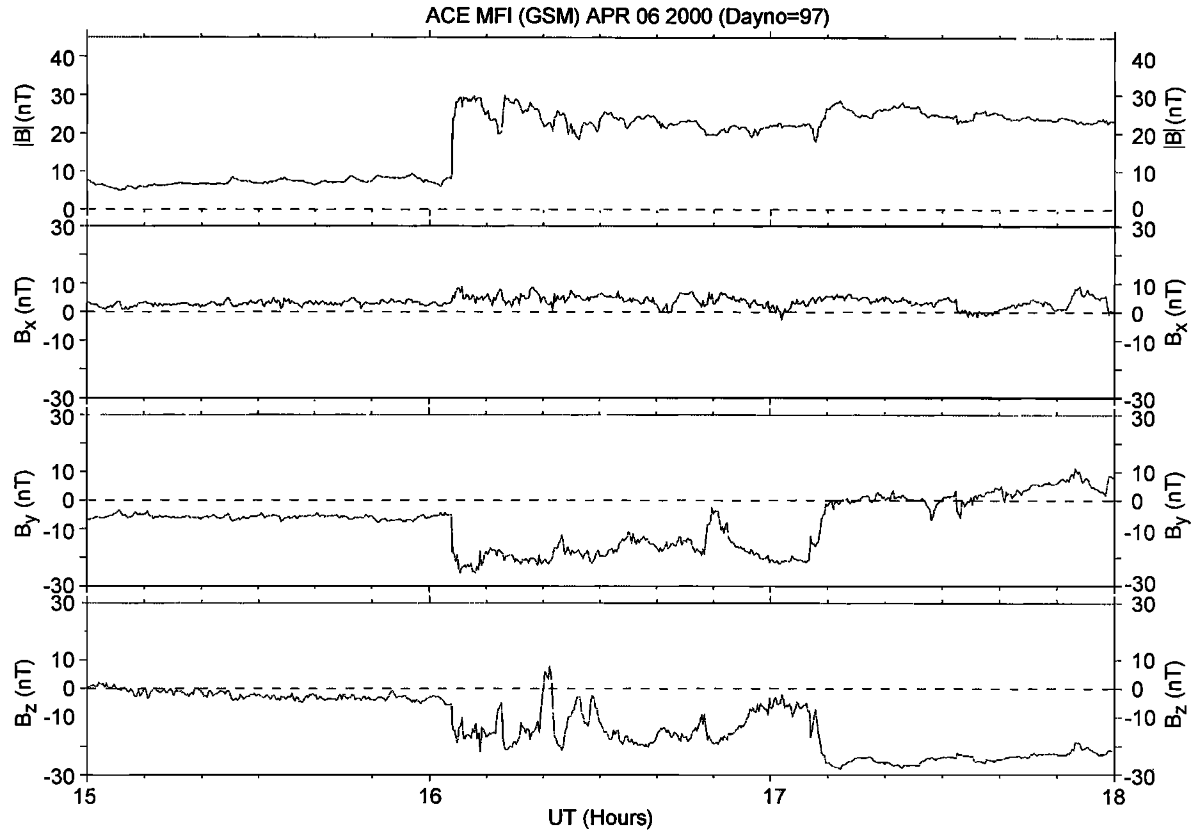

Figure 1. Stack plot of the components of the interplanetary magnetic field (IMF) measured at the ACE satellite for the period 1400–1800 UT on April 6, 2000. The satellite was located 225 R_E upstream of the Earth.

upstream at 1632 UT. Following a 1-hour period of variable B_y- and B_z-, the IMF rotated to a strongly southward orientation.

3. SuperDARN Nowcast of the High-Latitude Ionosphere

The SuperDARN radars operate around the clock and 365 days a year. The scan repeat rate is usually 2 min, although faster 1-min scans are increasingly being scheduled. On April 6, 2000, the scanning was performed at the 2-min rate. The radars ran the Common Mode program, which is optimal for mapping the large-scale convection. Internet links were available for six of the seven radars then constructed. The seventh (Stokkseyri) has since been equipped with an Internet connection. In this demonstration we will deviate from the real-time processing that was performed on this day by including the Stokkseyri data. We expect that future nowcasting at the JHU/APL web site will include real-time data downloads from all of the existing and planned radars.

For a discussion of the basic operation of a SuperDARN HF radar, see *Greenwald et al.* [1985, 1995]. In Appendix A the interested reader will find a discussion of some of the technical aspects of running the real-time connections. We also provide a guide to navigating the JHU/APL SuperDARN web site for space weather products. In the following we indicate the clickable links by enclosing their names in quotation marks (“ ”). Note that the longest delay in posting any of the real-time products to the web site is 8–10 min.

We begin the demonstration by highlighting some of the items that were available at the web site upon completion of the processing for the 1714–1716 UT scanning interval. These could have been viewed by a visitor to the JHU/APL SuperDARN homepage (http://superdarn.jhuapl.edu/) who had selected the link to “Real-Time Data”. By further selecting the link to the “Java Display Applet” and choosing “Kapuskasing” from the radar menu, the visitor could have generated the plots shown in Plate 2. The larger fan plot shows data from the Kapuskasing radar overlaid on a geographical map. The limits of the radar field of view are indicated by the black outline. The radar steps in azimuth through 16 beams (labeled 0–15), and samples backscatter returns within 45-km range gates. The plot is updated upon completion of each 7-s beam sounding, with a wait at the end of the scan to make up the 2-min scan period. The parameters that can be plotted with this applet are backscattered power, line-of-sight velocity, and spectral width; here, backscattered power is shown in the smaller fan plot, and line-of-sight velocity is shown in the larger. The extensive area of intense backscatter is due to ionospheric irregularities. These maps indicate the potential for auroral effects over this area.

It is useful to be able to place the instantaneous activity within the context of long-term trends. From the “Real-Time Data” page the user could have selected the link to “Time Series Plots”. This displays time series of power, velocity, and spectral width for each of the radars (a total of 24 plots for eight radars). The lower panel of Plate 2 shows a fragment of the plot pertaining to the Kapuskasing radar for the real-time processing that was completed with the scan ending at 1716 UT. Line-of-sight velocity is plotted as a function of range and time for a selected beam. We make out gray-coded bands within fairly stable range intervals. The gray coding indicates groundscatter, which arises from radar transmissions that are refracted by the ionosphere toward the ground and then reflected back to the radar along the same path. Although of no value for mapping ionospheric convection, groundscatter is a useful diagnostic of HF propagation conditions. From this plot it is clear that there was a sudden change in the backscatter beginning near 1640 UT. The stable, long-lasting groundscatter typical of propagation in the quiet midday ionosphere gave way to backscatter from ionospheric irregularities with large velocities. As we shall discuss, this change was due to the arrival of the shock in the ionosphere. The space weather effects in terms of auroral clutter and HF propagation in the high-latitude ionosphere were clearly dramatic.

The final set of real-time data displays is accessed from the "Real-Time Data" page through the link to "Convection Maps". This brings up a display of the current convection pattern. To illustrate the derivation of this important result, we show in Plate 3 a map of all the velocity information that was available for the scan ending at 1716 UT. This was produced by mapping the velocity data from the radars into a global grid of equal-area cells, as described by *Ruohoniemi and Baker* [1998]. The coverage extends across the dayside portion of the high-latitude ionosphere. The measurements from the Kapuskasing radar establish that the meridional component of the flows on the noon meridian was directed antisunward and reached magnitudes of 1 km s^{-1}. The convection pattern resolved from these data and posted to the web site is shown in Plate 4. The technique of fitting the data to an expansion of the electrostatic potential function, Φ, in terms of spherical harmonic functions is described by *Ruohoniemi and Baker* [1998]. The nowcast pattern incorporates certain refinements that are discussed by *Shepherd and Ruohoniemi* [2000].

Overall, the map shows a two-cell convection pattern with flow extending to relatively low latitudes on the dayside. As is commonly the case, the largest velocities are found in a narrow interval of MLT corresponding to the likely ionospheric footprint of the cusp/low–latitude boundary layer (LLBL) region. The largest magnitudes of electrostatic potential identify the centers of the dawn and dusk cells. The total cross polar cap potential variation, Φ_{PC}, is 108 kV. This comparatively high value indicates that energy and momentum are being transferred from the solar wind to the magnetosphere at an accelerated rate. As shown by *Shepherd and Ruohoniemi* [2000], the determination of Φ_{PC} is reasonably definitive when, as in this case, observations extend continuously from one potential extremum to the other. There are several significant space weather aspects of this result; the regions of high velocity are at greater risk for induced ground currents, the velocity and Φ_{PC} information are strong constraints on MHD space weather codes, and the convection pattern is an essential input for ionospheric modeling. The convection map itself is completely analogous to those of terrestrial weather where plasma velocity and electrostatic pressure function in the roles of wind velocity and barometric pressure, respectively.

The map includes a line that shows the result of fitting a boundary to the equatorward edge of the velocity measurements as explained by *Shepherd and Ruohoniemi* [2000]. The shape of this boundary is based on some findings of *Heppner and Maynard* [1987] regarding the location of the equatorward edge of the convection zone. The variable in the fitting is the size of the region enclosed by the boundary. We parameterize the result in terms of the crossing of the Heppner-Maynard (HM) boundary on the midnight meridian; in this case, $\Lambda_{HM} = 56°$. The boundary fitting is performed in real time and the result is used to constrain the solution for the convection pattern. The magnitude of Λ_{HM} itself is a useful way to characterize the latitudinal extent of irregularity occurrence. It is becoming clear through other studies that this boundary correlates well with the latitudinal limits of energetic particle precipitation. Thus the Λ_{HM} determination is a potentially valuable space weather product as it characterizes the spatial extent of auroral effects.

It will be noted that a global solution of the potential pattern is presented in the nowcast while the radar observations, though widespread, did not cover all sectors. As explained by *Ruohoniemi and Baker* [1998], data from a statistical convection model are used to supplement the radar velocity measurements. The weighting of the model data is selected to minimize the impact of the model while still stabilizing the solution over regions of no radar coverage [*Shepherd and Ruohoniemi*, 2000]. The model in routine use is that of *Ruohoniemi and Greenwald* [1996]. The selection of model data is keyed to the IMF conditions that are thought to prevail in the magnetosphere. For the nowcast result, the prediction of the effective IMF is based on the magnetic field data measured by the ACE satellite, with a delay to account for propagation to the ionosphere. As we shall discuss below, examination of the upstream satellite data and the SuperDARN data indicates a delay time τ_{AI} = 34 min between the solar wind at the position of ACE and effects in the ionosphere. Applying this delay to the scan interval that ends at 1716 UT, the IMF predicted to prevail in the ionosphere selects the statistical convection pattern for roughly equal B_y- and B_z- in the largest interval of IMF magnitude.

Another display that is possible from the link to "Convection Maps" is an animated replay (movie) of the convection patterns posted to the web site over the previous 2 hours. This allows for a dynamic review of the conditions in the high-latitude ionosphere. It is unfeasible to present here the entire run of 2-min images for the CME event of April 6, 2000; for a simulation of the movie that ran with the images collected over the 1600–1800 UT interval, see the "Event Studies" link on the JHU/APL SuperDARN homepage. Instead, we show in Plate 5 a montage of four maps that span the 1634–1700 UT period. The impact of the arrival of the solar wind shock is clear. Prior to 1640 UT the amount of irregularity scatter was limited and restricted to high latitudes. The estimated cross polar cap potential variation was 58 kV. The solution for the global pattern was dominated by the statistical model data, but there can be little doubt that the ionosphere was geomagnetically quiet. After 1640 UT there was a rapid increase in the amount of scatter and an equatorward leap in its extent. The convection pattern shows zones of high flow velocity. The total potential variation increased to 121 kV by the scan ending at 1700 UT. A user monitoring the web site would appreciate that a major geomagnetic disturbance had occurred in the high-latitude regions with obvious space weather consequences.

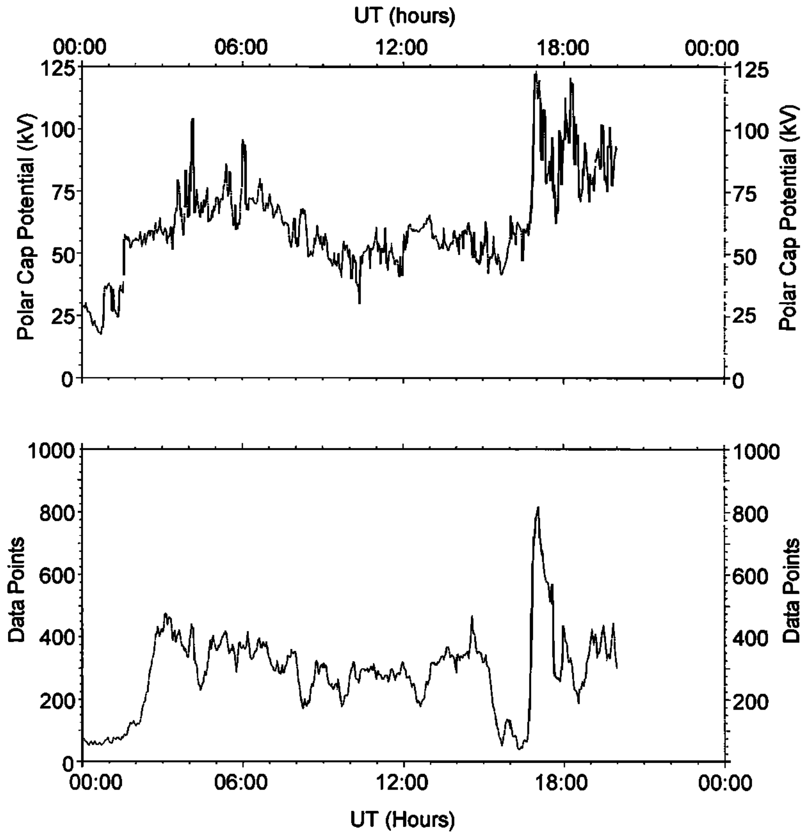

Figure 2. Time series plots for the scan ending at 2000 UT on April 6, 2000: (upper) the cross polar cap potential variation and (lower) the total number of velocity measurements available from the radars within the global grid.

Time series of some related parameters are displayed directly on the "Convection Maps" page. Figure 2 includes the plot for the cross polar cap potential variation that was posted upon completion of the processing for the scan ending at 2000 UT. The high-latitude convective flows were greatly intensified by the arrival of the shock and strongly southward IMF. (We have extended the period beyond the 1714 UT limit of our simulated nowcast in order to show the interesting oscillations in Φ_{PC} that followed the arrival of the shock.) The temporal evolution of Φ_{PC} is an important observational constraint for modeling the event with comprehensive space weather codes. (For this particular event we acknowledge that the expansion of the auroral zone was so great that a significant fraction of the convection pattern moved beyond the fields of view of the radars. When the velocity measurements are not sufficient to fix the potential variation between the likely positions of the cell centers, the nowcast determination provides a lower bound for Φ_{PC}.) The lower plot of Figure 2 shows the number of velocity measurements that were available from the SuperDARN radars within the grid cells. This indicates the overall intensity of irregularity activity.

As mentioned above, the radar data can be used to fix the delay from the passage of a perturbation in the solar wind at an upstream satellite to effects in the ionosphere. This delay is an important constraint for modeling the ionospheric response to solar wind factors. It also establishes the amount of advance warning that can be provided of space weather effects in the ionosphere on the basis of the satellite observations. We illustrate the determination of the delay from the Wind satellite to the ionosphere for the activity of April 6, 2000. Figure 3 shows a stack plot of satellite and radar data. (Although this exact plot is not available at the web site, its individual panels are displayed there or their contents can be reasonably inferred from review of posted material.) The plots of radar data include the time series of the total number of radar velocity measurements within the grid cells and of the largest velocity magnitude within each scan interval. The lowest frame shows a time series of the HM boundary, Λ_{HM}. A change in all three parameters was recorded with the scan beginning at 1640 UT. Comparing the times of transition in the satellite and radar data, we find delay values of τ_{AI} = 34 min for ACE and τ_{WI} = 6 min for Wind. It is important to note that the delay time discussed here is determined solely by observations and constitutes the effective lag between the onset of changes in the IMF at an upstream position and the onset of related changes in the ionosphere. It can be modeled as the sum of propagation times in the solar wind, the magnetosheath, and the ionosphere [e.g., *Ridley et al.*, 1998]. The empirical determination of the response time is useful for the testing and calibration of the various analyses that forecast space weather on the basis of upstream observations. In our own nowcasting we use it to select the statistical model data to be applied to the solution of the global convection pattern.

4. Summary

The high-latitude ionosphere is the site of geophysical activity with significant consequences for space weather. The coupling of the solar wind and magnetosphere can be monitored and studied advantageously through its ionospheric effects. In this paper we have demonstrated nowcasting of the high-latitude ionosphere with the SuperDARN HF radars. The JHU/APL SuperDARN web site promptly (<1 min) posts some items pertaining to the extent of irregularity backscatter and the conditions of HF propagation. With a delay of 8–10 min, the web site includes a map of the global convection pattern derived from a combination of velocity measurements from the radars and statistical model data. This constitutes in essence a map of the space weather in the high-latitude ionospheric plasma convection.

Here we list some of the products of space weather interest that are available from this nowcasting facility: (1) local maps of backscatter from the individual radars that contain information on the conditions of HF propagation and the potential for auroral effects; (2) time series of data from the individual radars permitting review of local conditions; (3) line-of-sight velocity data mapped into a global grid suitable for the testing and calibration of MHD codes; (4) a map of the global convection pattern, describing the overall conditions within the high-latitude ionosphere in terms of plasma velocity and the potential distribution, useful for the evaluation and adjustment of MHD codes and the running of ionospheric models; (5) a measure of the spatial extent of auroral effects through the determination of the equatorward boundary of the zone of irregularity backscatter; (6) time series of the global convection pattern, cross polar cap potential variation, and other parameters; and (7) the time delay from upstream satellites to effects in the ionosphere which may be determined by review of posted materials limits the amount of advance warning that is possible and provides a test for solar wind propagation models.

The nowcast convection pattern that we have described satisfies a critical need for timely, comprehensive information on ionospheric electric fields. The prevailing conditions can be gauged from the size and character of the convection pattern, and the mapping can provide the electric field inputs that are required to model the evolution of effects in the ionosphere and neutral atmosphere. Ultimately, the MHD codes being developed to predict space weather must account for the electric field component of solar wind–magnetosphere–ionosphere coupling as manifested in these observations, and these codes will likely need to incorporate the nowcast information to make accurate forecasts.

Additional refinements of the space weather products provided by the JHU/APL SuperDARN web site are planned. These include the routine incorporation of convection velocity measurements from incoherent scatter radars. The interested reader might also want to draw on the extensive records of observations that are archived there. Data downloads and

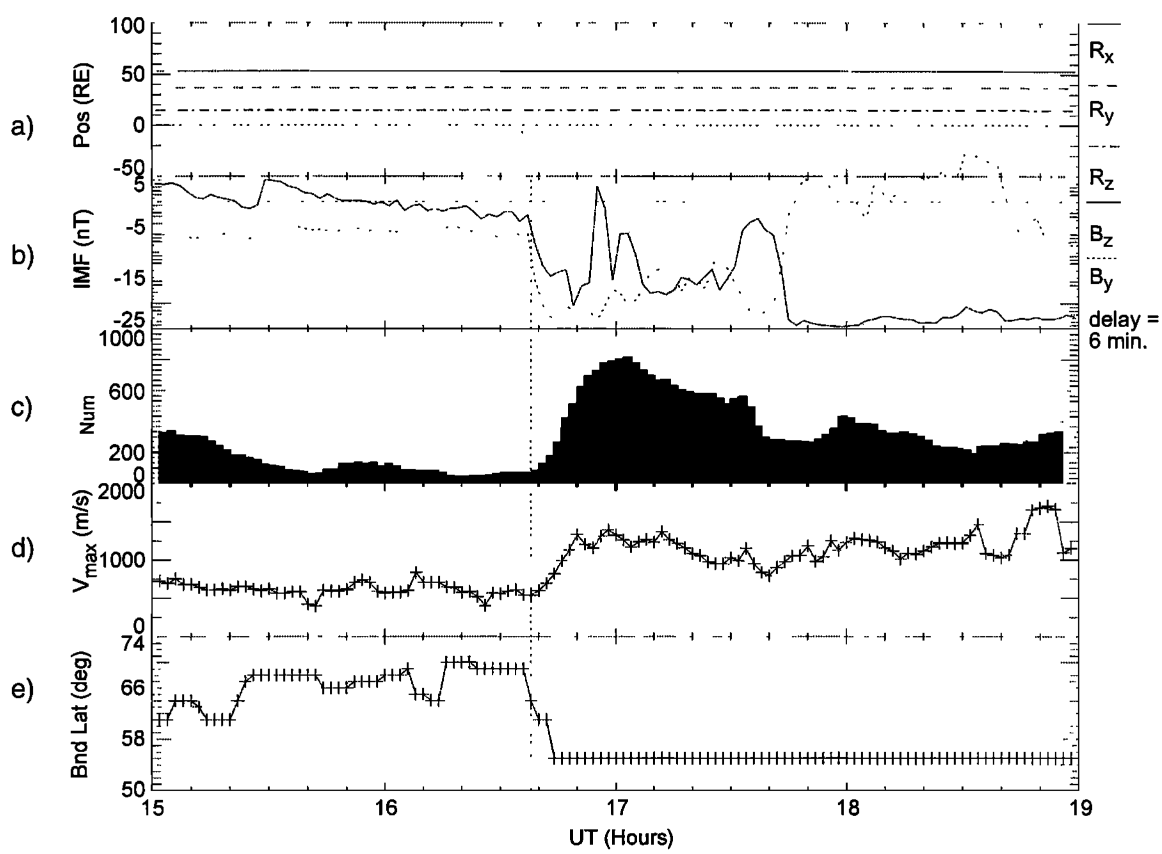

Figure 3. Stack plot of satellite and radar data that serves to identify the effective delay between observations at the satellite and related effects in the ionosphere. The panels show, in descending order from the top, (a) the position of the Wind satellite, (b) the components of the IMF in the GSM plane (*z* is solid, *y* is dashed), (c) the total number of velocity measurements from within the grid, (d) the largest line-of-sight velocity magnitude recorded within the grid, and (e) the latitude of the crossing of the Heppner-Maynard boundary (Λ_{HM}, as defined in the text) with the midnight meridian.

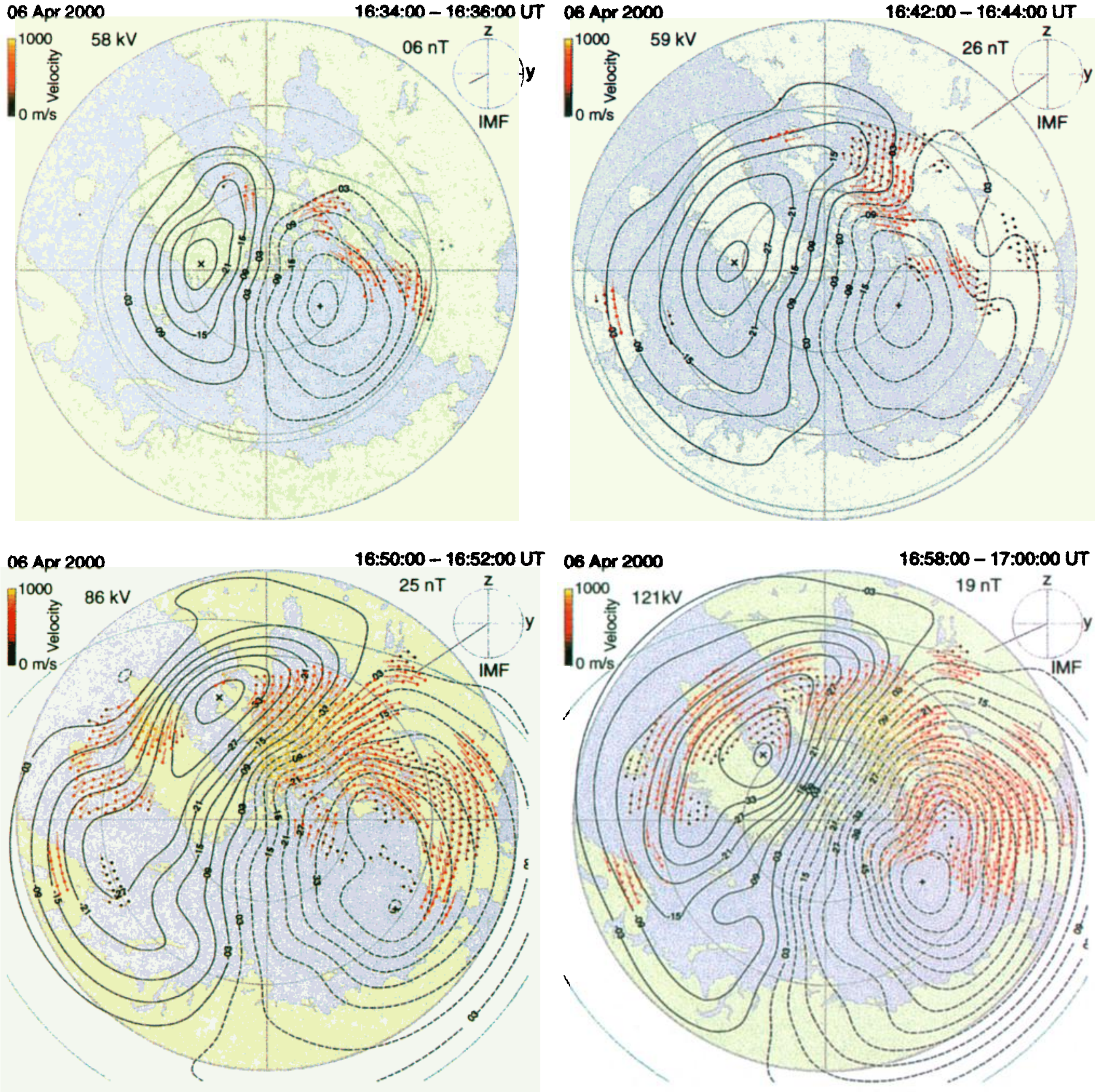

Plate 5. Time series of the convection patterns spanning the arrival of the solar wind shock in the ionosphere on April 6, 2000. These images are excerpted from the nowcast movie that was available with the completion of the real-time processing for the scan ending at 1716 UT.

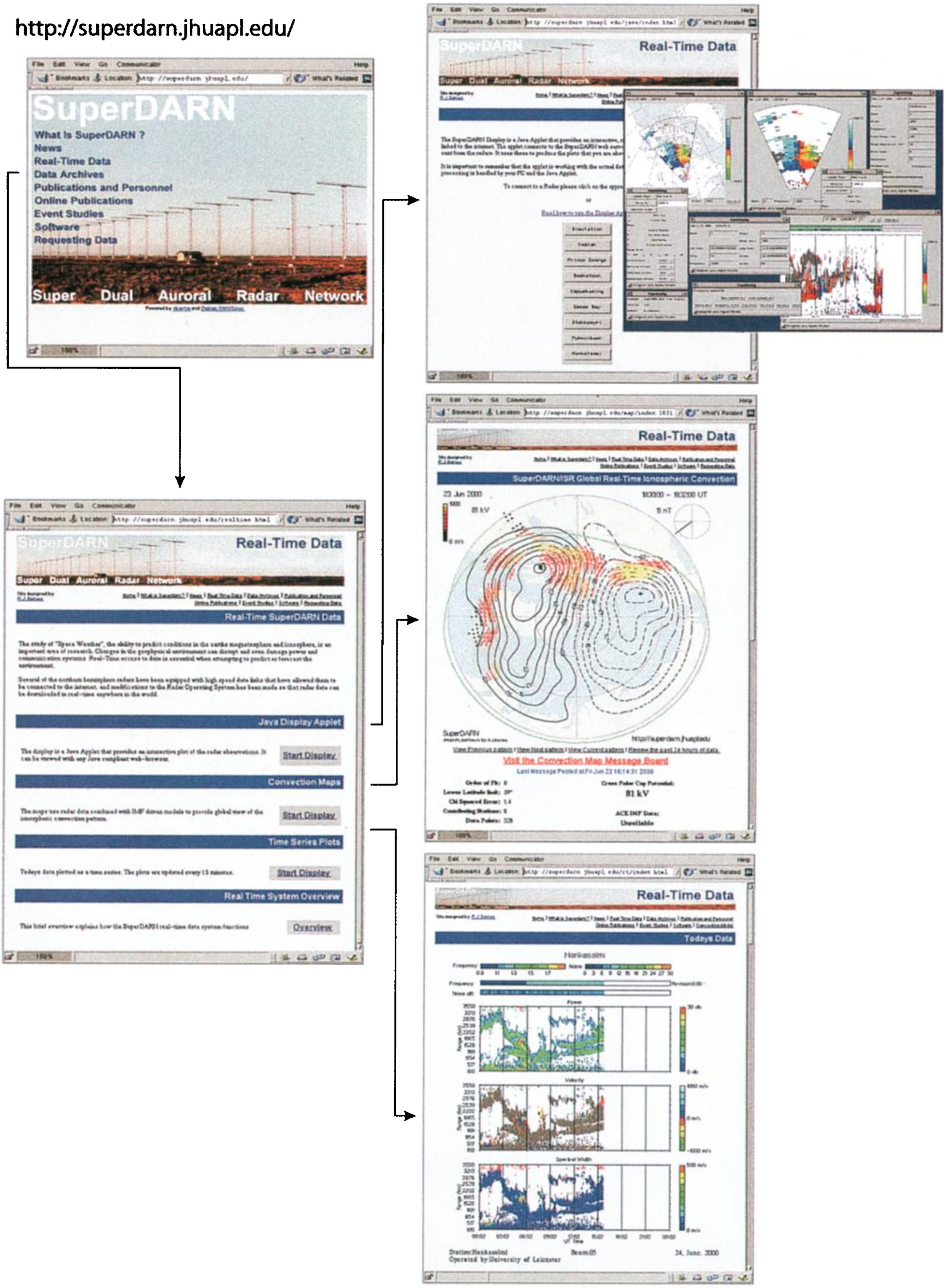

Plate 6. Guide to the real-time products available at the JHU/APL SuperDARN web site.

customized analysis of particular events can be requested. We welcome comments and suggestions for further improvement.

Appendix A

The generation of real-time products at the JHU/APL SuperDARN web site depends on the timely transmission of data from the remote HF radar sites to computers at JHU/APL. The data transmission system consists of two parts, the remote servers that provide real-time data feeds from the radar sites and local clients that receive the data at JHU/APL. Here we describe some technical aspects of the real-time operation of SuperDARN and provide a guide to the nowcast products.

The remote server is run as part of the Radar Operating System at each radar site and uses the standard Transmission Control /Internet Protocol (TCP/IP) to transfer data to one or more remote clients. The program listens for connection requests from remote clients. Once a client has been connected, the program will receive a packet of data each time the radar completes a sounding. This is an example of "server push," as the client passively waits to receive data. By contrast, the Web operates using "client pull," where data are requested by a web browser from an otherwise passive server.

The main real-time data products available at JHU/APL are the global ionospheric convection maps and the Java Display Applet. The network connections to the radars are fairly low bandwidth, and if too many clients tried to connect to the radars, the links would quickly become clogged. To solve this problem there is a special program run at JHU/APL that acts as both client and server. It acts as a client by connecting to a radar site and receiving data, and it acts as a server by relaying that data to one or more other clients. This means that only one connection is required to a radar site, and the entire network load is moved to the system at JHU/APL.

A necessary step in generating the convection maps is to clean up the raw data received from the radar sites. Two-minute blocks of data are filtered to remove noise and to extract only those observations associated with ionospheric irregularities. The observations are mapped to a global grid as described by *Ruohoniemi and Baker* [1998]. The result of this processing is a text file containing the line of sight velocities of the ionospheric scatter observed during a 2-min scan. These files, one for each radar, are combined together to create a single file containing all the observations of the whole network. Data from other sources, such as incoherent scatter radars, are added to the SuperDARN data when available. The velocity data are fit to an expansion of the electrostatic potential in terms of spherical harmonic functions, and the resulting global convection pattern is displayed on the web page.

We consider the time delay in presentation of the real-time products. The Java Display Applet is updated with the transmission of each data packet from the radar, where a packet contains the summary information for a single beam sounding. This is quite fast, and the delay of the Applet behind current time is usually less than a minute and often barely more than the 7-s beam sounding period. The generation of the convection map, on the other hand, requires downloads of data for three consecutive scans, including the scan after the scan under consideration. Also, downloads are sought from all of the radars, and the connections for some may be slow or inactive. To cope with this, the processing software waits a designated period to capture the data required for the designated scan. If incomplete, it times out and proceeds to generate a pattern. The total delay resulting from these considerations is usually 8–10 min. (This figure can be reduced through certain economies and trade-offs should the need arise.) It will also be appreciated that the nowcast patterns are provisional, in that they might not be based on all the velocity measurements that will eventually become available or use the optimal settings of the various fitting parameters.

The real-time products are accessible from the JHU/APL SuperDARN homepage through the link to "Real-Time Products". Plate 6 provides a guide for accessing specific items. Note that the real-time convection map is currently updated every minute although the usual scan period is 2 min.

Acknowledgments. This work was supported by NSF grants ATM-9613847 and ATM-9819891 and by NASA grants NAG5-8361 and NAG5-8037. Operation of the SuperDARN radars in the Northern Hemisphere is supported by the national funding agencies of the U.S., Canada, the U.K., France, and Japan. We gratefully acknowledge NOAA/SEC and CDAWeb for access to solar wind data.

Janet G. Luhmann thanks Marc R. Hairston and another referee for their assistance in evaluating this paper.

References

Greenwald, R. A., et al., DARN/SuperDARN: A global view of high-latitude convection, *Space Sci. Rev.*, *71*, 763-796, 1995.

Greenwald, R. A., K. B. Baker, R. A. Hutchins, and C. Hanuise, An HF phased-array radar for studying small-scale structure in the high-latitude ionosphere, *Radio Sci.*, *20*, 63-79, 1985.

Heppner, J. P., and N. C. Maynard, Empirical high-latitude electric field models, *J. Geophys. Res.*, *92*, 4467-4489, 1987.

Rich, F. J., and H. M Hairston, Large-scale convection patterns observed by DMSP, *J. Geophys. Res.*, *99*, 3827-3844, 1994.

Ridley, A. J., G. Lu, C. R. Clauer, and V. O. Papitashvili, A statistical study of the ionospheric convection response to changing interplanetary magnetic field conditions using the assimilative mapping of ionospheric electrodynamics technique, *J. Geophys. Res.*, *103*, 4023-4039, 1998.

Ruohoniemi, J. M., and K. B. Baker, Large-scale imaging of high-latitude convection with Super Dual Auroral Radar Network HF radar observations, *J. Geophys. Res*, *103*, 20,797-20,811, 1998.

Ruohoniemi, J. M., and R. A. Greenwald, Statistical patterns of high-latitude convection obtained from Goose Bay HF radar observations, *J. Geophys. Res.*, *101*, 21,743-21,763, 1996.

Shepherd, S. G., and J. M. Ruohoniemi, Electrostatic potential patterns in the high latitude ionosphere constrained by SuperDARN measurements, *J. Geophys. Res.*, *105*, 23,005-23,014, 2000.

Weimer, D. R., Models of high-latitude electric potentials derived with a least error fit of spherical harmonic coefficients, *J. Geophys.*, *100*, 19,595-19607, 1995.

Yeoman, T. K., R. V. Lewis, S. E. Milan, and M. Watanabe, An interhemispheric study of the ground magnetic and ionospheric electric fields during the substorm growth phase and expansion phase onset, *J. Geophys. Res.*, *104*, 14,867-14,877, 1999.

R. J. Barnes, R. A. Greenwald, J. M. Ruohoniemi, and S. G. Shepherd, The Johns Hopkins University Applied Physics Laboratory, 11100 Johns Hopkins Road, Laurel, MD 20723-6099. (mike_ruohoniemi@jhuapl.edu)

(Received June 30, 2000; revised September 7, 2000; accepted September 26, 2000.)